Earth and Planetary Science Letters 375 (2013) 280–290

Contents lists available at ScienceDirect

Earth and Planetary Science Letters

journal homepage: www.elsevier.com/locate/epsl

The stabilisation and transportation of dissolved iron from high temperature hydrothermal vent systems

J.A. Hawkes [a,b,*], D.P. Connelly [a], M. Gledhill [b], E.P. Achterberg [b]

[a] National Oceanography Centre Southampton, Southampton SO14 3ZH, UK
[b] Ocean & Earth Science, University of Southampton, National Oceanography Centre Southampton, Southampton SO14 3ZH, UK

ARTICLE INFO

Article history:
Received 28 November 2012
Received in revised form
8 May 2013
Accepted 28 May 2013
Editor: G. Henderson
Available online 4 July 2013

Keywords:
iron
ligand
colloid
hydrothermal plume
CLE–ACSV
speciation

ABSTRACT

Iron (Fe) binding phases in two hydrothermal plumes in the Southern Ocean were studied using a novel voltammetric technique. This approach, reverse titration–competitive ligand exchange–adsorptive cathodic stripping voltammetry, showed that on average 30 ± 21% of dissolved Fe in the hydrothermal plumes was stabilised by chemically labile binding to ligands. The conditional stability constant (log K'_{FeL}) of the observed complexes was 20.61 ± 0.54 (mean ± 1 SD) for the two vent sites, intermediate between previous measurements of deep ocean ligands (21.4–23; Kondo et al., 2012) and dissolved weak estuarine ligands (< 20; Gerringa et al., 2007).

Our results indicate that approximately 7.5% of all hydrothermal Fe was stabilised by complexation with ligands. Furthermore, 47 ± 26% of the dissolved Fe in the plume existed in the colloidal size range (0.02–0.2 μm). Our data suggests that a portion (~7.5%) of hydrothermal Fe is sufficiently stabilised in the dissolved size fraction (< 0.2 μm) to make an important impact on deep ocean Fe distributions. Lateral deep ocean currents transport this hydrothermal Fe as lenses of enhanced Fe concentrations away from mid ocean ridge spreading centres and back arc basins.

1. Introduction

Iron (Fe) is an important and often limiting micronutrient in the world's oceans (Martin and Fitzwater, 1988). Dissolved Fe (DFe) concentrations in the surface ocean are typically < 0.3 nM, and range between ~0.2 and 1.2 nM in the deep ocean (> 1000 m) where Fe is buffered by strong organic ligands (De Baar and De Jong, 2001; Hunter and Boyd, 2007). The study of the sources, sinks and speciation of Fe is crucial to our understanding of the transport and bioavailability of this element. The supply of Fe to the world's oceans is poorly constrained, with atmospheric dust, rivers, sediments and remineralisation of sinking particles forming the main sources (De Baar and De Jong, 2001). Hydrothermal sources of stable DFe have recently been considered due to several observations of high DFe concentrations in the deep ocean close to tectonic spreading centres, often in regions containing elevated (hydrothermally sourced) ^{3}He (Klunder et al., 2011; Kondo et al., 2012; Nishioka et al., 2013; Wu et al., 2011).

Iron is highly enriched in high temperature hydrothermal fluids as it is leached from host rocks during hydrothermal circulation of seawater. End-member concentrations can range from < 2 μM (e.g. Menez Gwen, Mid Atlantic Ridge, Douville et al., 2002) to > 10 mM Fe (e.g. Edmond vent site, Central Indian Ridge, Gallant and Von Damm, 2006). The total (dissolved and particulate) contribution of Fe to the deep ocean by high temperature hydrothermal vents is estimated to be 7.2–450 Gmol Fe yr^{-1} (Baker et al., 1993; Bennett et al., 2008; Elderfield and Schultz, 1996; Tagliabue et al., 2010), while the total DFe inventory of the ocean is estimated to be 800–1600 Gmol (De Baar and De Jong, 2001). The impact of hydrothermal vents on global DFe distributions is still poorly understood due to the high spatial (German and Von Damm, 2004) and temporal (e.g. Butterfield and Massoth, 1994; Campbell et al., 1988) variability in hydrothermal fluid emissions, and the complexity of Fe speciation and removal in seawater.

A large portion of hydrothermal Fe is deposited close to vent sources as sulphide mineral phases (Mottl and McConachy, 1990) and the remaining Fe(II) is rapidly oxidised and forms oxyhydroxide particles (Feely et al., 1987; German et al., 1990; Field and Sherrell, 2000). However, Fe is often observed to oxidise or precipitate more slowly in hydrothermal plumes than predicted by laboratory kinetic studies, and this has been attributed to interaction of Fe(II) with organic matter and sulphides (Statham et al., 2005; Toner et al., 2009; Wang et al., 2012) and also stabilisation of Fe(III) in the dissolved phase by complexation with organic ligands

* Corresponding author at: National Oceanography Centre Southampton, Southampton SO14 3ZH, UK.
E-mail address: j.hawkes@noc.soton.ac.uk (J.A. Hawkes).

0012-821X
http://dx.doi.org/10.1016/j.epsl.2013.05.047

(Bennett et al., 2008). Fine Fe containing particles (or "colloids") are also considered to contribute to the observed enhanced dissolved (usually <0.2 or <0.45 μm) Fe concentrations (Field and Sherrell, 2000), and both oxy-hydroxide (Fe(III)) colloids and pyrite nano-particles (Fe(II)) have been detected in hydrothermal vent systems (Sands et al., 2012; Yucel et al., 2011).

The only study that has considered DFe complexation in hydrothermal plumes was restricted to analysis of samples from the edges of the distal plume. It was suggested that a small percentage (~4%, 0.3 Gmol yr^{-1} globally) of hydrothermal Fe was transported to the deep ocean as DFe (Bennett et al., 2008). Here, we used a new voltammetric speciation technique to enable investigation of Fe speciation in the core of two hydrothermal plumes, where Fe is potentially saturating organic complexes. We also considered the differences between 'dissolved' Fe (<0.2 μm), "soluble" Fe (<0.02 μm) and "chemically labile" Fe (the Fe fraction that is complexed with an added electro-active ligand)—thus combining the study of physical and chemical speciation of Fe for the first time in hydrothermal plume systems.

The two vent sites (E2 and E9N; Rogers et al., 2012) are situated on the East Scotia Ridge (ESR) in the Southern Ocean and were sampled in 2010 for DFe ligand complexes. E9N was re-visited in 2011 to collect samples to determine the colloidal Fe (DFe minus soluble Fe) distributions. Sampling was conducted over a range of seawater to vent fluid mixing ratios (~200–160,000). However, due to the rapid dilution of vent fluid in hydrothermal buoyant plumes, the sample matrix (major ions, pH, temperature, etc.) was only ever slightly different from ambient seawater. Our aim was to investigate whether Fe in hydrothermal plumes is complexed by "ligand" phases that are co-diluted with Fe from the vent or by ambient ligands already present in the local deep seawater. We discuss the implications of our results for the transport of hydrothermal Fe to the deep ocean.

2. Materials and methods

2.1. Study areas

The East Scotia Ridge (ESR) is a back-arc basin spreading centre between the Scotia Plate and the South Sandwich Plate in the Atlantic sector of the Southern Ocean. Spreading at the ESR was initiated over 15 Ma ago and is currently proceeding at an intermediate rate of ~65–70 mm yr^{-1} (Bruguier and Livermore, 2001). It consists of 10 segments, E1–E10, of which two, E2 and E9, host hydrothermal activity (Rogers et al., 2012). The local deep ocean water was Weddell Sea Deep Water (WSDW), as defined by a potential temperature of −0.7 to 0.2 °C (Naveira-Garabato et al., 2002), see Supplementary information. At E2, the WSDW is partially mixed with Lower Circumpolar Deep Water (LCDW) which has a characteristic potential temperature of 0.2–0.7 °C.

The E2 site (located at 56.089°S, 30.317°W) is bathymetrically rough with large vertical displacements running north to south (Fig. 1). The E9 site (located at 60.043°S, 29.982°W) is comparatively flat and represents a local topographic elevation, a result of magmatic inflation in the centre of the ridge (Bruguier and Livermore, 2001). The principle geochemical features of the two sites are outlined in Table 1. Our samples were taken from hydrothermal plumes of the "Dog's Head" chimney at E2 and the "Black and White" chimney of the northern section of the E9 site (E9N) (Fig. 1).

The Fe concentrations in the end-member fluids were intermediate in a global context (see Supplementary information), and the concentration of hydrogen sulphide was high (6.7–9.5 mM, cf. Mid Atlantic Ridge range: 0.6–6.0 mM; Douville et al., 2002). This is likely due to the influence of the fluid rich subduction plate on the mantle at back arc basin sites (de Ronde et al., 2001; Baker et al., 2008), and probably leads to the early precipitation (as sulphides) of a higher portion of DFe (Baker and Massoth, 1987). Overall, the sites offer a typical environment in which to conduct a study into hydrothermal Fe seawater reactions.

2.2. Hydrothermal plume detection and sampling

Samples were collected and filtered at sea during two cruises on the RRS *James Cook* in the Southern Ocean, along the East Scotia Ridge (ESR) in 2010 (E2 and E9N; cruise JC042) and 2011 (E9N only; cruise JC055). The hydrothermal plume was detected and sampled using a Seabird +911 conductivity, temperature and the depth (CTD) profiler system that was mounted on a titanium frame with 24 trace metal clean 10 l OTE (Ocean Test Equipment) water sampling bottles. The frame was also equipped with a light scattering sensor (LSS) and a bespoke Eh detector (Ko-ichi Nakamura).

The buoyant part of the hydrothermal plume was identified by positive temperature and particle anomalies and a negative Eh anomaly, while the neutrally buoyant plume was identified by a positive particle anomaly and negative temperature and Eh

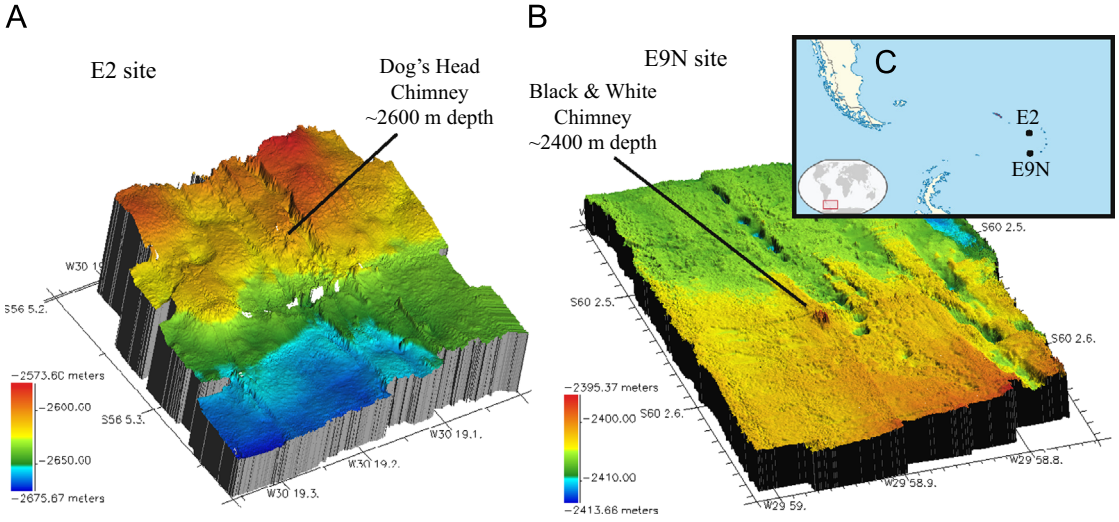

Fig. 1. A and B: Bathymetry of the E2 site surrounding the "Dog's Head" chimney and E9N site surrounding "Black and White" chimney, from which the sampled plumes emanate. C: Location of the E2 and E9N sites in Southern Atlantic Ocean. Scale bars = 30 m.

Table 1
Hydrothermal and seawater end-member composition at E2 and E9N.

	E2 (Dog's Head)	E9N (Black and White)	East Scotia Sea (> 1800 m depth)
Max temperature (°C)	353	383	~0
pH (total scale, at 25 °C for vent fluids)	2.9	3.4	7.9
Cl^- (mM)	536	98	541
H_2S (mM)	6.7	9.5	0
DFe (M)	1.28×10^{-3}	0.80×10^{-3}	1.7×10^{-9}
DMn (M)	2.05×10^{-3}	0.20×10^{-3}	0.5×10^{-9}
H_2S:Fe	5.2	11.9	0
Dissolved O_2 (μmol kg^{-1})	N/A	N/A	200 (E2), 172 (E9)
Dissolved inorganic carbon (DIC) (μmol kg^{-1})	> 7815 (Highest measured)	N/A	2256
Total alkalinity (TA) (μmol kg^{-1})	−920	−580	2360
Total P (μmol kg^{-1})	~0	~0	2.15 (E2), 2.21 (E9)
Total Si (mmol kg^{-1})	17.7	8	0.12

Vent fluid data from Rogers et al. (2012) and James et al. (in preparation).
N/A = not assessed.

anomalies at 350–400 m above the seafloor (Fig. 2). The plumes appeared to change position and intensity daily (based on the LSS anomaly, see various CTD profiles in Fig. 2), probably due to variations in deep water current speed, direction and tidal cycles. The ESR does not have an axial valley, so there is no seafloor feature to confine the neutrally buoyant plume, allowing dispersal in varying directions according to deep ocean currents. As a result, the hydrothermal plumes can be sampled at many levels of dilution over small spatial areas above the two vent fields.

Four "near vent" plume samples were taken from diffuse flow areas and the first few metres of buoyant plume rise (identified visually) using five 1.2 l OTE bottles on the remotely operated vehicle (ROV) *Isis*. The five bottles were closed simultaneously and combined (6 l) into one large OTE bottle and treated identically to the CTD profiler bottles, as described below.

A background CTD cast was also conducted at 59°40.898 S, 33°06.181 W, where no water column anomalies were observed. This site had a similar water depth (~2500 m) to the hydrothermal sites, but was > 50 km to the west of the ESR, and presumably beyond any strong influence of the dispersing plume. Samples were taken at depths equivalent to those of the buoyant and neutrally buoyant plumes at E9N (2350 and 2000 m, respectively). The background deep ocean Fe concentrations averaged 1.7 nM in 6 OTE bottles (range 0.94–2.59 nM), which is consistent with other studies further to the east and west in deep waters of the Southern Ocean (0.4–0.6 nM at 0°W (Klunder et al., 2011), 0.4–2.8 nM at 6°W (Loscher et al., 1997) and 1.6–4.2 nM close to the South Orkney islands at 48.23°W (Nolting et al., 1991)).

2.3. Assessment of in-situ pH using alkalinity and dissolved inorganic carbon

Dissolved inorganic carbon (DIC) and alkalinity were measured using a VINDTA 3C analyser (Miranda). Nutrients (phosphate and silicate) were measured by Seal QuAAtro, and these data were used to calculate in situ pH using CO2sys (Lewis and Wallace, 1998).

2.4. Filtration and analysis of size fractions of Fe and Mn

Dissolved (500 ml, < 0.2 μm) and particulate (> 0.2 μm) metals were separated by filtration of seawater using a polycarbonate membrane filter (0.2 μm, Whatman) under gentle pressure using filtered oxygen free nitrogen gas. Separate aliquots of filtered seawater were frozen for reverse titration–competitive ligand exchange–adsorptive cathodic stripping voltammetry (RT–CLE–ACSV) analysis (see below). The entire bottle contents (10 l) was filtered for particulate material, and the OTE bottles were shaken before the filtration finished to attempt to recover all material. It is still possible that larger material settled to the bottom of the OTE bottle (beneath the tap fixture) and was not recovered. On cruise JC055 (2011) at the E9N site, "soluble" (< 0.02 μm) metals were separated by filtration using syringe filters (25 mm, Anotop; Whatman) by peristaltic pumping using a flow rate of < 1 ml min^{-1}. We note that the actual cut-off size of these filters may be significantly smaller than 0.02 μm (Chen and Wang, 2004). The following wash and sampling was conducted through two syringe filters (0.1 μm and 0.02 μm) in series: a pre-wash of 30 ml pH 2 deionised water (MQ, Millipore, > 18.2 mΩ cm^{-1}; acidified with ultrapure HCl) followed by rinsing with deionised water for at least 4 h before sampling, then 20 ml of sample seawater was flushed through the filters and discarded and 40 ml of sample seawater was collected. pH 8 adjusted deionised water was filtered in the same way, and the extracted Fe concentration was below the detection limit (2.33 nM). Colloidal Fe was assumed to be the difference in 'dissolved' and 'soluble' Fe, as in other studies (e.g. Wu et al., 2001).

All filtered seawater samples from the CTD profiler were acidified to pH 1.9 with sub-boiled nitric acid (Optima, Fisher Scientific). On shore, dissolved metals were pre-concentrated from 100 ml of sample (30 ml for soluble Fe) by mixed ligand extraction (Bruland et al., 1979) and analysed using inductively coupled plasma mass spectrometry (ICP-MS; Thermo Scientific X-series) analysis. Deionised water was used to determine the procedural blank (Mn = 0.08 nM, Fe = 0.62 nM), the limit of detection (L.O.D.) (3σ of blank, $n = 27$) for Mn and Fe was 0.14 and 0.70 nM, respectively. For the lower volume soluble (< 0.02 μm) Fe samples, the L.O.D. was 2.33 nM. The vast majority of dissolved and soluble sample concentrations were higher than the L.O.D. for Fe. Accuracy was assessed using NASS-5 certified seawater (measured Fe: 3.74 ± 0.62 nM ($n = 7$), certified 3.70 ± 0.625) and precision was determined with NASS-5 and an in-house standard (8.5–16.6% depending on Fe concentration). The near vent samples taken by the ROV *Isis* had very high concentrations of Fe and Mn and were directly analysed by ICP-MS (X-series, Thermo Fisher Scientific) following dilution (100 ×) into 3% sub-boiled nitric acid containing an internal standard of Be and In (20 ppb and 10 ppb).

Particulate material (from 10 L of seawater) was stored frozen on the polycarbonate membrane filters, which were cut in half with ceramic scissors, and one half of each was digested for 3 days at 150 °C in sub-boiled concentrated nitric acid in a PTFE bomb (German et al., 1991) (the other half was stored for additional analysis). Filter material remaining after the acid digestion was soaked with a further 10 ml of sub-boiled concentrated nitric acid. The acid was removed by drying in a PTFE bomb on a Teflon coated hot plate set at 90 °C, then the dried samples were diluted in 3%

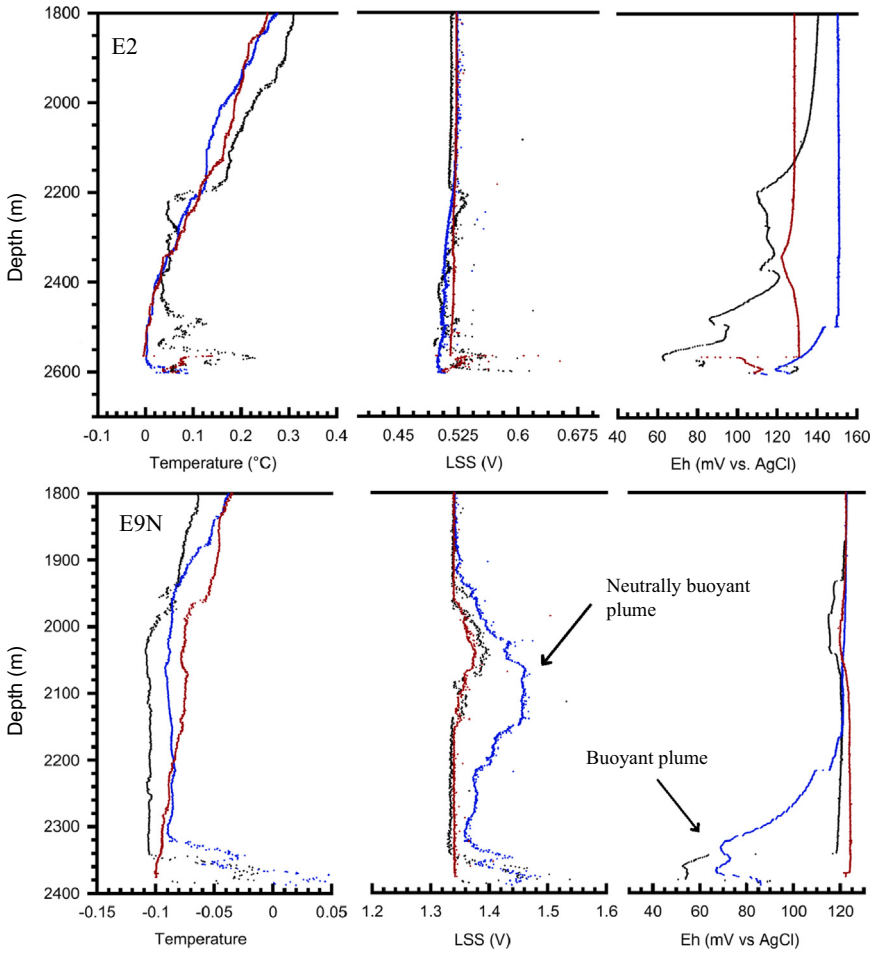

Fig. 2. Temperature, LSS and Eh profiles at depth > 1800 m for three CTD casts (indicated by different colours) at different times but similar positions from E2 and E9N. The negative temperature anomaly in the neutrally buoyant plume is due to entrainment of colder seawater from deeper in the water column. The light attenuation anomaly is due to the presence of particles, and the negative Eh anomaly due to the presence of reduced species (HS^-, Mn^{2+}, Fe^{2+}). (For interpretation of the references to colour in this figure legend, the reader is referred to the web version of this article.)

sub-boiled nitric acid containing internal standard and analysed by ICP-MS. The L.O.D. (3σ of average blank filter) for Mn and Fe was 1.4 and 78.4 pM, respectively.

2.5. Determination of Fe speciation by RT–CLE–ACSV

The forward titration technique is typically used to determine Fe binding ligands in seawater but is not appropriate for use in environments with excess Fe or large quantities of inert DFe (Laglera and van den Berg, 2009; Gledhill and Buck, 2012), and as such has limited use in hydrothermal environments (Bennett et al., 2008). The reverse titration–CLE–ACSV approach allows analysis of ligands at equal or lower concentrations than chemically labile Fe (Hawkes et al., 2013). The theory has been previously described for analysis of Cu, Fe(II) and Fe(III) binding ligands (Nuester and van den Berg, 2005; Statham et al., 2012; Hawkes et al., 2013).

Samples (250 ml) were filtered (0.2 μm pore size, polycarbonate, Whatman) and stored frozen at ambient pH. On shore they were defrosted at 4 °C (close to their in-situ temperature) and shaken vigorously before preparation of the titration. The titration was carried out and labile Fe (Fe_{NNmax}) was determined as described in Hawkes et al. (2013).

The near vent samples taken using the ROV *Isis* all had DFe concentrations in excess of 100 nM (range 290–1430 nM). The method had to be modified in these cases because the data manipulation relies on [NN] being in large excess over [Fe_{NNmax}]. These samples were diluted in deionised water to three different salinities (20×, 10× and 5× dilution) and analysed in the same way as described above (with a 120 s deposition time). The change in salinity was not found to affect the calculated value of K'_{FeL}, but did affect the calculated (i.e. zero dilution) concentrations of Fe_{NNmax} and L–which increased at lower salinity. The full data can be found in the Supplementary information; here we present the calculated average result for K'_{FeL} and values for [Fe_{NNmax}] and [L] calculated from the 5× dilution.

2.6. Data fitting

The experimental data were all fitted to Eq. (1) using a non-linear regression code package in the open source software R. This process has been described previously (Hawkes et al., 2013).

$$X = \frac{[FeNN_3]}{Fe_{NNmax}} = (1-j)\frac{\alpha_{FeNN_3}}{\alpha_{FeNN_3} + \alpha_{Fe'}} + j\frac{\alpha_{FeNN_3}}{\alpha_{FeNN_3} + \alpha_{Fe'} + ([L]K'_{Fe'L}/1 + K'_{FeL}[Fe^{3+}])} \quad (1)$$

where X is the measured peak height (i_p) divided by the maximum achievable peak height (i_{pmax}, where all NN labile Fe (Fe_{NNmax}) occurs as $Fe(NN)_3$) and j is the fraction (0–1) of Fe_{NNmax} bound to ligands L (i.e. L/Fe_{NNmax}). [L] and $K'_{Fe'L}$ are fitted to the experimental data, [Fe^{3+}] is calculated from the resulting mass balance of Fe_{NNmax} (Nuester and van den Berg, 2005), α_{Fe} is $10^{9.80}$ at pH 7.90

(Hawkes et al., 2013) and $\alpha_{FeNN_3} = \beta_{FeNN_3}[NN]^3$. β_{FeNN_3} is 5.12×10^{26} under our typical experimental conditions (Hawkes et al., 2013), and the value was adjusted to account for salinity (Gledhill and van den Berg, 1994) in the high Fe samples that were diluted.

3. Results

The deep Scotia Sea was ~0 °C and had dissolved oxygen concentrations of 200 μmol kg^{-1} (E2) and 172 μmol kg^{-1} (E9N). Dissolved inorganic carbon (DIC) was 2256 μmol kg^{-1} and alkalinity 2360 μmol kg^{-1}. From these and nutrient data (Table 1), we calculated a local (in-situ) pH_{tot} of 7.9.

The temperature, LSS and Eh profiles for the two hydrothermal plumes E2 and E9N are shown in Fig. 2. The E2 neutrally buoyant plume (NBP) had a weaker LSS anomaly that was generally more variable than for the plume of E9N. These differences may be due to differences in Fe oxy-hydroxide and sulphide abundance (which have different light attenuation properties) rather than vent output (Baker and Massoth, 1987). The plume rise was ~400 m at E2 and ~350 m at E9N, both of which are consistent with the obtained end-member temperatures (Table 1) and water column densities (data not shown) using the plume rise model of Turner (1973).

Iron binding phases were successfully determined within the applied detection window using RT–CLE–ACSV in samples from both the E2 and E9N plumes, including the near vent samples. The ligand concentrations ranged from 2 to 18 nM in the plume samples, and the average ligand concentration was 25 ± 15% of the DFe concentration at E2 and 39 ± 27% of DFe at E9N. The stability constant (log K'_{FeL}) of the Fe–ligand complexes averaged 20.51 ± 0.45 (mean ± 1 SD) at E2 and 20.79 ± 0.65 at E9N (see Fig. 3 for three examples of titration data). No trend in log K'_{FeL} was observed with dilution of the vent fluid (Fig. 4), including in the near vent samples, indicating that the binding strength of the Fe–ligand complexes was not related to their concentration or distance from the vents.

The E2 plume contained a far greater concentration of Fe in the dissolved and particulate phases than E9N (Fig. 5), but the E2 and E9N sites were not different in log K'_{FeL} or L:Fe ratio (as demonstrated by a large overlap of values), suggesting these factors may be independent of DFe and total Fe concentrations between sites. The percentage of CFe (0.02–0.2 μm) in the DFe pool at E9N ranged between 5% and 82%, and averaged 47 ± 25%. The concentration of CFe was highest in the middle (47% of DFe) and lower (82%) portion of the NBP compared with the top (26%)—which contained a larger portion of soluble Fe (Fig. 6). The labile Fe concentration (Fe_{NNmax}, occasionally higher than L) averaged 26 ± 15% of DFe at E2 and 47 ± 27% of DFe at E9N.

4. Discussion

4.1. Fe speciation in the hydrothermal plumes

The typical Fe concentrations in the plume were low in comparison with many other vent sites which have been studied for Fe speciation (e.g. the 5°S Mid Atlantic Ridge plumes, Bennett et al., 2008; the Edmond vent plume, Sands et al., 2012; the Rainbow vent plume, Edmonds and German, 2004), and this may be the result of relatively high sulphide concentrations in the East Scotia Ridge vent fluids, removing a large portion of the Fe in the early buoyant plume (Field and Sherrell, 2000; Mottl and McConachy 1990; Klevenz et al., 2011). This was particularly the case at E9N, where low chloride concentrations suggest a vapour phase was sampled after sub-seafloor phase separation. This process favours gases such as hydrogen sulphide over cations such as Fe, and may also lead to a higher proportion of Fe being precipitated as sulphides in the early plume.

Our results showed that a portion of DFe was complexed by ligands in all parts of the hydrothermal plumes. Iron binding phases were typically equal to (or more concentrated than) Fe_{NNmax}, and Fe_{NNmax} was generally substantially less than DFe (Fig. 5), showing that not all DFe was electrochemically labile under our experimental conditions. The observed Fe_{NNmax} fraction is operationally defined by the concentration of added ligand used (here: 40 μM NN) and the binding strength of NN to Fe (β_{FeNN_3}; 5.12×10^{26} mol^{-1}). Natural complexes with a binding coefficient α_{FeL} ($[L]K'_{FeL}$) which are much greater than α_{FeNN_3} ($\beta_{FeNN_3}[NN]^3$) or

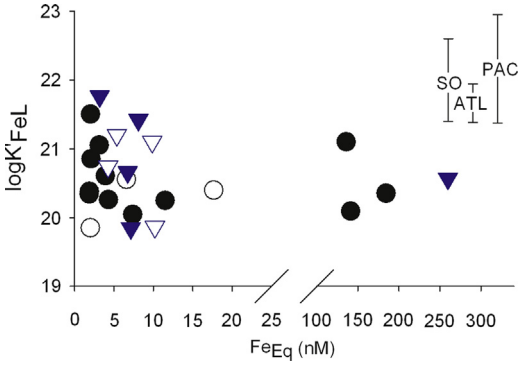

Fig. 4. log K'_{FeL} plotted against electrochemically labile Fe (Fe_{NNmax}) in the plume and near vent samples. We found no trend in stability constant with Fe concentration. Black circles: E2, blue triangles: E9N. Data which were poorly fitted by the RT–CLE–ACSV model are included as unfilled symbols. The range of results previously reported in the (non-hydrothermal) deep sea from the Southern Ocean (SO), Atlantic (ATL) and Pacific (PAC) are shown for comparison (Boye et al., 2010; Croot et al., 2004; Cullen et al., 2006; Kondo et al., 2012; Rue and Bruland, 1995).

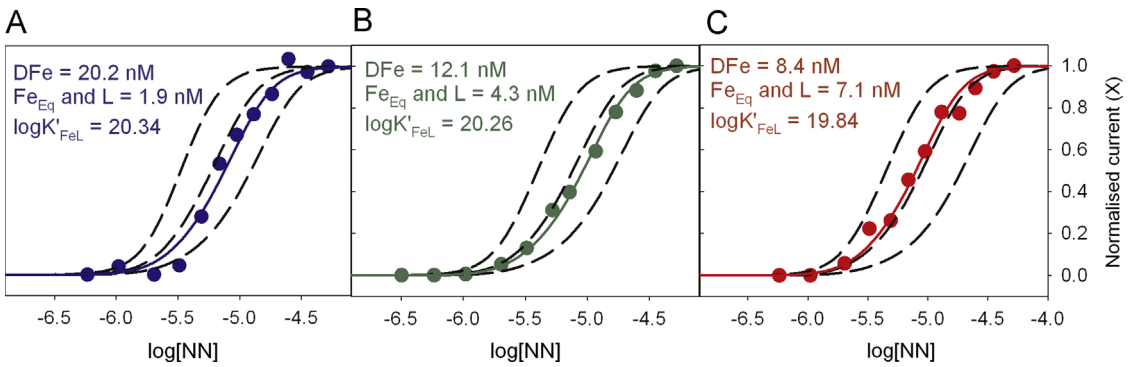

Fig. 3. RT–CLE–ACSV data and model outputs for three samples: A: E2 buoyant plume, B: E2 neutrally buoyant plume, C: E9N buoyant plume. Circles show the experimental data and the solid lines the model fit. Dashed lines show the model fit for log K'_{FeL} = 19, 20 and 21 (left to right) for the same concentration of Fe and L. The R package for fitting data is available in the Supplementary information.

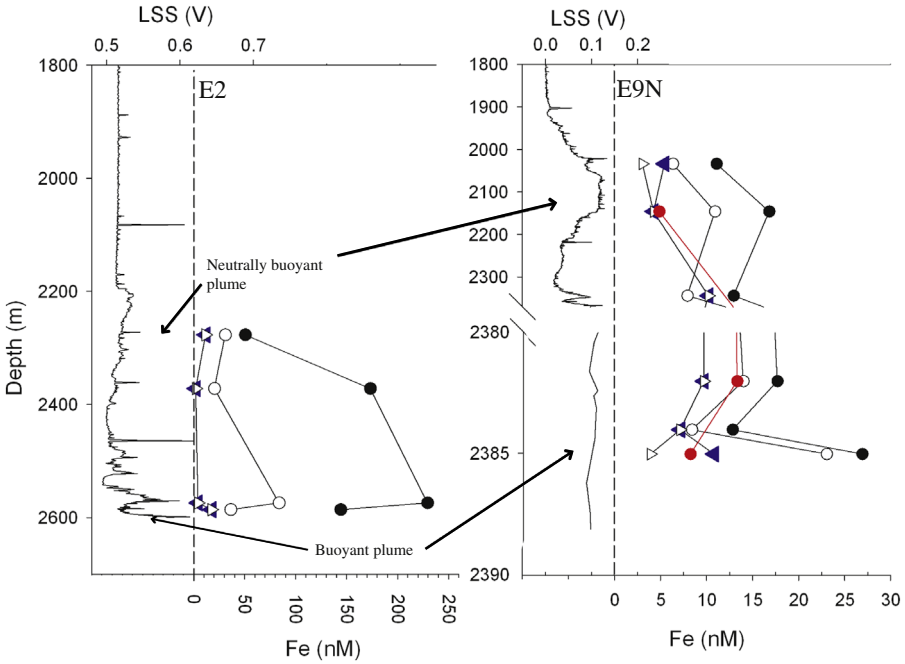

Fig. 5. Example profiles of LSS and Fe at E2 and E9N (Station CTD424). Filled black circles: total (dissolved+particulate) Fe, unfilled black circles: dissolved Fe, filled red circles: soluble Fe, filled blue triangles: Fe_{NNmax}, unfilled black triangles: Fe binding ligands. Note the break in scale on the depth axis for E9N. (For interpretation of the references to colour in this figure legend, the reader is referred to the web version of this article.)

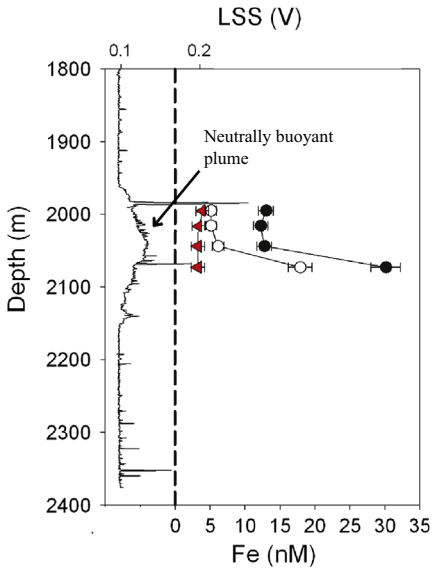

Fig. 6. Depth profile of Fe size fractions in the neutrally buoyant plume at E9N (Station CTD428). Filled black circles: total (dissolved+particulate) Fe, unfilled black circles: dissolved Fe, red triangles: soluble Fe. (For interpretation of the references to colour in this figure legend, the reader is referred to the web version of this article.)

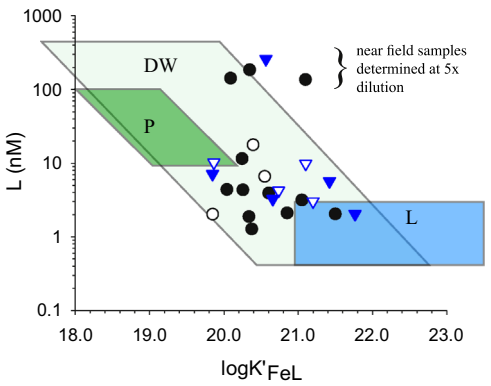

Fig. 7. Concentrations of Fe binding phases plotted against stability constant at E2 and E9N. In addition to the data (black circles: E2, blue triangles: E9N), typical ranges of the same factors are shown for L in the deep Southern Ocean (Boye et al., 2001; Croot et al., 2004) and for 'P' the weak ligand suggested to exist in high concentrations in an estuary in Gerringa et al. (2007). The detection window 'DW' is also shown for varying ligand concentrations. (For interpretation of the references to colour in this figure legend, the reader is referred to the web version of this article.)

have similar strength to the inorganic species of Fe (e.g. hydrolysis products) will not be detected. This may include sulphide ligands (e.g. SH^-) and the very weak class of ligands previously detected in estuarine environments (Gerringa et al., 2007), which is a comparable marine environment (i.e. with steep chemical gradients; Fig. 7). Ligands that are too strong to be detected by this technique may also have been important in stabilising Fe—and crystalline colloidal phases and nano-pyrite particles are likely to constitute the 'inert' Fe pool.

The log K'_{FeL} values averaged 20.51 at E2 and 20.79 at E9N, 20.61 combined, and these are lower than most of the complexes reported for the deep ocean (Fig. 4; Boye et al., 2010; Croot et al., 2004; Cullen et al., 2006; Kondo et al., 2012; Rue and Bruland, 1995). Marine Fe binding ligands exist in an un-interrupted continuum of Fe binding strengths, and those detected may only depend on the detection window of the technique used (Hiemstra and van Riemsdijk, 2006; Hassler et al., 2013). In this study our detection window (α_{FeL}~$10^{9.8}$–$10^{13.7}$) is bound by the concentration of Fe in the sample and by the range of $FeNN_3$ concentrations that can practically be determined. We constrain this detection window by requiring 80% of i_{pmax} to be reached over the course of the titration for data fitting purposes. Our detection window is lower than that commonly applied in forward titrations (α_{FeL}~$10^{12.6}$–$10^{14.6}$). However, previous studies have reported an inverse relationship between ligand binding strength and ligand concentration (Hiemstra and van Riemsdijk, 2006; Stockdale et al., 2011), so that at higher Fe concentrations, such as those observed

in this study, weaker ligands become more important for stabilising Fe in solution. The ligand phases reported here for hydrothermal plumes are indeed weaker than typically detected open ocean ligands, and make up the weakest of the "L_2" set of ligands which are often observed in the deep ocean (Gledhill and Buck, 2012; Hunter and Boyd, 2007; Laglera and van den Berg, 2009; Rue and Bruland, 1995). However, differences between the forward and reverse titration techniques may preclude direct comparison of the obtained K'_{FeL}. The important implications of our findings are that some portion of hydrothermal DFe was found to be sufficiently labile to exchange with NN and that the obtained K'_{FeL} did not appear to change as the plumes developed or between the two sites.

4.2. The effect of Fe oxidation state, pH and hydrothermal constituents on the in-situ speciation

The in-situ speciation of Fe is likely to be different than that detected under our experimental conditions, in which the temperature, pH and pressure were all modified and some reduced species (e.g. Fe^{2+}, $H_2S_{(aq)}$) were given time to oxidise. The ambient pH in the deep Scotia Sea was 7.90 (very similar to the buffered pH) but temperature was ~23°C colder, thereby reducing the inorganic side reaction coefficient (Schlosser et al., 2012; Hassler et al., 2013). The samples were also frozen, potentially allowing aggregation of colloidal phases (Schlosser et al., 2011). The hydrothermal fluid constituents of the plume may also affect the Fe speciation, as the fluid is acidic and has a very different ionic composition. However, only hydrothermal constituents that are highly enriched ($> 10^5 \times$) over seawater have significantly higher concentrations in the plume, particularly once it has been emplaced to neutral buoyancy (~$10^4 \times$ dilution; Lupton et al., 1985). As a result, only pH is sufficiently different from ambient seawater to have an important affect on the Fe speciation. The range of pH of the plume samples in this study (calculated from dissolved inorganic carbon and total alkalinity; Lewis and Wallace, 1998) was 7.5–7.9 (total pH scale). The lowest near vent sample had an in-situ pH of 7.0. The solubility and speciation of Fe(III) is critically dependent on pH (Gledhill et al., 1998; Millero et al., 2009; Shi et al., 2010) due to competition for Fe^{3+} by L^- and OH^-. At lower pH Fe hydrolysis is decreased, Fe is more soluble (Liu and Millero, 2002) and more free Fe^{3+} is available for ligand complexation. Ligands that have acidic binding groups that are not protonated in seawater form stronger complexes, whereas no change in conditional stability constant is observed for protonated ligands (Shi et al., 2010). When the samples are buffered and free Fe^{2+} is allowed to oxidise over the course of preparation, they are driven towards thermodynamic equilibrium and more typical seawater conditions. The experimental results are therefore more representative of the eventual products of the reaction of hydrothermal fluid with seawater rather than the speciation at the exact time and location of sample collection in the plume.

4.3. Source and nature of FeL

Our results showed that the amount of bound Fe (FeL) increased with dissolved Mn, indicating that the hydrothermal vents act as a source of FeL (Fig. 8). The observation that FeL is diluted with the plume and thus appears to have a plume source raises questions about the nature of FeL.

Firstly we consider the hydrothermal Fe binding phases in vent plumes to be classically organic in nature (e.g. Bennett et al., 2008) with a 1:1 Fe:L binding ratio. The source of these ligands is unlikely to be directly from the high temperature vent, but rather lower temperature diffusive areas of venting which are found adjacent to high temperature hydrothermal vents and may

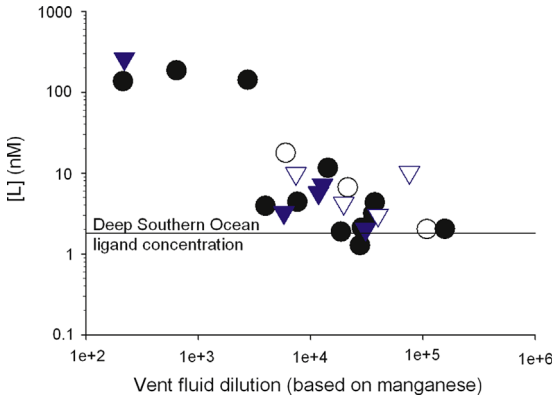

Fig. 8. Concentration of Fe binding phases (L) plotted against dilution of pure vent fluid with seawater (based on dissolved manganese). Black circles: E2, blue triangles: E9N. Data which were poorly fitted by the RT–CLE–ACSV model are included as unfilled symbols. Note that [L] for the near vent samples was calculated from a sample which was diluted 5 × with deionised water. Typical deep southern ocean ligands are shown as a horizontal line (from Croot et al. (2004)). (For interpretation of the references to colour in this figure legend, the reader is referred to the web version of this article.)

contribute up to 98% of the total hydrothermal mass flux (Baker et al., 1993). Higher concentrations of dissolved organic carbon (DOC) compared with ambient deep seawater and end-member fluid (i.e. 48 μM compared with 36 μM and 15 μM, respectively; Lang et al., 2006) have been observed in these areas. It has been suggested that this material is more labile (more reactive and with a greater variety of functional groups) than the typically recalcitrant deep ocean DOC (Karl, 1995; Lang et al., 2006), and may have the functionality to chelate vent sourced DFe (Bennett et al., 2008). Various studies have considered the distribution and activity of bacterial populations in hydrothermal plumes (e.g. de Angelis et al., 1993; Bennett et al., 2013; Karl, 1995) usually concluding that bacteria metabolise methane in hydrothermal plumes, producing particulate and dissolved organic matter (POM, DOM). Some of the resulting DOM may have a capacity to bind Fe, and, furthermore, some bacteria may actively produce dissolved organic ligands as a mechanism for sequestering Fe (Gledhill and Buck, 2012). While the actual amount of organic matter produced by bacteria from methane is probably as low as that entrained from diffusive areas of venting (Bennett et al., 2013), these mechanisms may well be important in the chemically rich plume. If the DOC composition reported in Lang et al. (2006) are typical and a maximum of 98% of the hydrothermal input to the plume was from lower temperature venting then the ratio of hydrothermal C to Fe in the plume could be up to 1.4:1 (Eq. (2)).

$$\frac{[C_{plume}]}{[Fe_{plume}]} = \frac{[C_{HT}]x_{HT} + [C_{LT}]x_{LT}}{[Fe_{HT}]x_{HT} + [Fe_{LT}]x_{LT}} \quad (2)$$

where x is the fractional mass proportion of high temperature (HT) and low temperature (LT) fluids. This level of DOC input (< 1 μM) would not typically be detected by DOC analysis; e.g. Bennett et al. (2011, 2013) and could help to support some stabilisation of Fe. However, the actual concentration of ligand molecules which could be provided (requiring several carbon atoms) via this mechanism may be low, and there is some dispute about the amount of diffuse water that is entrained into buoyant plumes (German et al., 2010). It is therefore unlikely that FeL is dominated by compounds that can be considered classically organic.

A second explanation for the apparent presence of increased FeL levels in the hydrothermal plumes is that deep ocean water contains a relatively high concentration (10–100 nM) of weak organic or inorganic ligands, which are not typically detected by cathodic stripping voltammetry techniques (Croot and Heller,

2012; Gerringa et al., 2007). After storage and overnight equilibration of our samples, any such ligand phase (which would often be in excess of Fe_{NNmax}) would enter into binding competition with the added ligand for Fe_{NNmax}. This may explain the low stability constant detected in our experiments. If this is the case, the relative kinetics of Fe ligand binding (Croot and Heller, 2012; Witter et al., 2000; Wu and Luther, 1995) and Fe precipitation may play a crucial role in the amount of Fe actually complexed in hydrothermal plumes before hydrolysis and precipitation.

Sulphide ligands may also be important in these environments, where reduced sulphur species can temporarily exist in the presence of oxygenated seawater. The ligand bisulfide (SH^-) has complexing capacity for several metals including Fe(II) (Luther et al., 1996) but the stability constant for $FeSH^+$ ($\log \beta_1 = 5.1–5.5$) and Fe_2SH^{3+} ($\log \beta_2 = 10.1–11.8$) are weak in comparison to the ligands detected in this study (Luther and Ferdelman, 1993; Luther et al., 1996). Additionally, the Fe and sulphide in some kinetically labile complexes may oxidise over the course of sampling, storage and equilibration during the preparation of the titration. These complexes may therefore be important in the early stages of venting, where Fe and S^{2-} are in similar concentrations, but less important as the plume disperses into the deep sea and under our analytical laboratory conditions.

Iron sulphide compounds (e.g. pyrite nanoparticles) are now recognised to be important in the dissolved phase in hydrothermal plumes (Yücel et al., 2011), particularly in high sulphide vent sites. These particles probably form a large part of the "inert" and possibly some of the "labile" DFe fraction, although the reactivity of Fe(II) in nano-particulate pyrite and organic matrices (Yucel et al., 2011; Toner et al., 2009) is unknown. The chemical reactivity of Fe sulphide phases deserves further attention, given their apparent pervasiveness in hydrothermal environments.

Lastly, we consider a mechanism similar to the "onion" concept of Mackey and Zirino (1994), which describes Fe binding involving aggregates with multiple layers of coordination bonds. A portion of Fe may form weakly bound aggregates (colloids) that are electrochemically labile, but are not technically bound in individual coordination bonds with singular "organic ligands" as described in other theories (Croot and Johansson, 2000; Gledhill and van den Berg, 1994; Rue and Bruland, 1995). Colloids form when dissolved metal ions rapidly coagulate together by sorption, due to the attractive electrical charge of ionic surfaces (Honeyman and Santschi, 1989). Colloidal phases form more quickly than larger, filterable particles because coagulation between larger particles proceeds at a slower rate compared with surface sorption (Farley and Morel, 1986; Honeyman and Santschi, 1989, 1991). Iron also has a strong tendency to form amorphous colloidal phases with organic matter (Hunter and Liss, 1982; Moore and Braucher, 2008; Mosley et al., 2003), and this process would be particularly likely to occur in turbulent hydrothermal plumes where physical and chemical gradients are steep. This theory is supported by our observations of enhanced concentrations of Fe colloids in the E9N plume that corresponded well with the average concentration of Fe binding phases (colloids = 47% and L = 39% of total DFe). We assume here that hydrothermal CFe is made up of a mixture of amorphous oxy-hydroxide colloids (Sands et al., 2012), nano-pyrite clusters (Luther and Rickard, 2005; Yucel et al., 2011) and colloidal-sized FeL (e.g. Boye et al., 2010; Cullen et al., 2006). Although the "onion" model as described by Mackey and Zirino considers adsorption of metals onto organic colloids in the euphotic zone of the oceans, we consider this theory useful for explaining our results. Future Fe speciation studies in hydrothermal settings should aim to separate truly soluble FeL species from all dissolved FeL species as previously reported (Boye et al., 2010; Chen and Wang, 2004; Cullen et al., 2006) in order to more closely assess the role of colloids in stabilising hydrothermal Fe inputs.

Our observation that a large portion of hydrothermal Fe rapidly forms colloids in the plume is consistent with experimental studies where high concentrations of Fe were added to organic rich seawater (Boye et al., 2005; Nishioka et al., 2005). Observations of natural Fe inputs (rivers, dust deposition) to seawater also show that a large portion of new Fe forms colloids (Benoit et al., 1994; Bergquist et al., 2007; Sañudo-Wilhelmy et al., 1996). Coastal upwelling of Fe rich water also leads to a large variation of partitioning between soluble and colloidal Fe due to redox and biological processes (Ussher et al., 2010).

The mechanism of stabilisation of Fe by 'onion' aggregation (Mackey and Zirino, 1994) we propose here is consistent with theory and observations made to date. This mechanism of Fe binding may be much more widespread than just in hydrothermal systems, and could be a crucial control on Fe distributions in many parts of the ocean.

4.4. The transport and fate of Fe from hydrothermal systems

Regardless of the nature of FeL, our data suggest that a large portion (30%) of DFe in hydrothermal plumes exists in a chemically labile form that is available for transportation by deep ocean currents. In the E2 and E9N plumes, this corresponds to 10.1% of total hydrothermal Fe (E2), 9.0% (E9N) or $9.72 \pm 7.2\%$ (combined), based on the following formula:

$$\text{mean}\% \text{ Fe stabilised} = \sum_x \left(\frac{FeL_x}{\text{TFe}_{\text{hydrothermal}}} \cdot \frac{\text{TMn}_{\text{hydrothermal}}}{\text{Mn}_x} \times 100 \right) \quad (3)$$

This relies on conservative mixing of Mn, which may be considered a maximum estimate as some Mn is oxidised by bacteria and on the surfaces of particles in the plume (Cowen and Li, 1991; Davies and Morgan, 1989; Dick et al., 2009), and Mn may also react with dissolved sulphide to form sulphide particles (Breier et al., 2012). If only 60% of the vent emitted Mn remained in the NBP samples (and 100% in the buoyant plume samples; Klinkhammer et al., 1986), the amount of hydrothermal Fe stabilised for the two sites may be revised to $7.5 \pm 7.5\%$. This result has a high level of uncertainty due to the complexity, irregularity and turbulent nature of hydrothermal plumes (Lupton et al., 1985).

The figure may also be considered as a minimum estimate, as other (kinetically inert) phases are also available for transport, and may in fact be scavenged less quickly from solution onto particles due to their lower reactivity. We have little experimental information about the nature of Fe species in the dissolved phases that are not part of the Fe_{NNmax} fraction, and these species merit further investigation. We assume here that a large portion is purely inorganic (colloidal) Fe oxy-hydroxides (Field and Sherrell, 2000; Sands et al., 2012) and pyrite nano-particles (Yucel et al., 2011).

Regarding the behaviour of Mn, we noticed that in samples which were strongly diluted ($> 20{,}000\times$) with seawater, the DFe concentrations appeared to tend towards a concentration of approximately 5–10 nM above background (Fig. 9). The implications of this were that in the aged plume, DFe concentrations might be depleted at a lesser rate than DMn. Owing to the very changeable deep ocean currents in this study area, the NBP that we sampled was an effluent cloud that dispersed in all directions and may be several hours or even days old. Because Mn does not tend to form colloidal phases in hydrothermal plumes (Sands et al., 2012; colloidal = 0.1–0.4 μm) and is not complexed by organic ligands, it will be oxidised and not remain in the effluent for as long as stabilised DFe. The main consequence of this result is that the stated order of dilution in Fig. 8, which is determined from Mn concentrations, should be considered as a maximum estimate, particularly in more diluted samples.

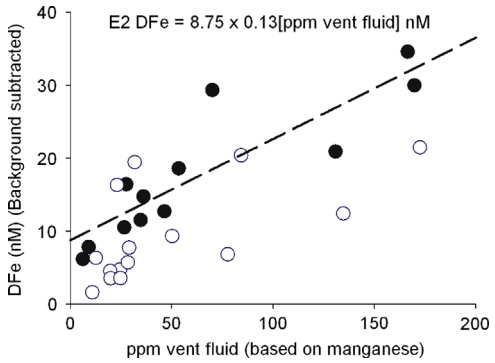

Fig. 9. Dissolved Fe plotted against vent fluid concentration in seawater (ppm) in the neutrally buoyant plumes for E2 (filled black circles) and E9N (unfilled blue circles). The dilution is based on dissolved manganese, which is often used as a conservative tracer. The dashed line shows a regression for the E2 samples, which tend to 8.75 nM Fe above background rather than zero as predicted. The E9N samples showed a much higher degree of variation, which was also found in the RT–CLE–ACSV experiments, possibly indicating more complicated and diverse Fe speciation. (For interpretation of the references to colour in this figure legend, the reader is referred to the web version of this article.)

Colloidal (or smaller) material is not expected to settle in seawater (according to Stokes' settling laws) (Yucel et al., 2011), and is therefore likely to be transported over large distances away from hydrothermal plumes by deep ocean currents. The likelihood of further aggregation of colloidal and FeL type complexes is low (Honeyman and Santschi, 1989) due to the extremely low concentrations involved (<100 nM) as the plume disperses and particle/colloid concentrations decrease (Field and Sherrell, 2000). This stabilisation of DFe in the NBP is clearly important to the transport of Fe and the significance of hydrothermal plumes as a source of Fe to the deep ocean. It is likely that hydrothermal vents indeed produce the lenses of enhanced DFe concentrations that have been observed in the deep ocean (Klunder et al., 2011; Kondo et al., 2012; Nishioka et al., 2013; Wu et al., 2011), and may also supply large quantities of colloidal Fe to the deep ocean (Bergquist et al., 2007; Wu et al., 2001). Interestingly, our results differ from those of Nishioka et al. (2013) in that we see a large contribution of CFe to the DFe pool, whereas they found a large influx of SFe from hydrothermal sources. The different observations may be due to small differences in Fe(II) oxidation rates or vent fluid sulphide concentrations, which control partitioning between soluble Fe(II) and colloidal Fe(III) in early stages of plume development (Field and Sherrell, 2000). In our study area, the likely destination of stabilised vent Fe is towards the east on the Antarctic continental shelf after movement along the circumpolar current and upwelling to the surface ocean (Marshall and Speer, 2012). A volcanic eruption from the South Sandwich Island Arc has previously resulted in pumice being transported around the entire Southern Ocean (Sutherland, 1965; Coombs and Landis, 1966; Risso et al., 2002).

Our estimation that 7.5% of hydrothermal Fe is stabilised by Fe binding phases is slightly higher than the 4% reported by Bennett et al. (2008). These workers suggested that hydrothermal vents could provide 11–22% of deep ocean Fe. Since then, attempts have been made to incorporate the hydrothermal contribution of DFe to global oceans into numerical models (e.g. Sander and Koschinsky, 2011; Tagliabue et al., 2010). It is important to note that to date we have little understanding of what constrains the portion of hydrothermal Fe that is stabilised for transport from an individual vent site. Hydrothermal fluids vary in Fe composition over more than 5 orders of magnitude (see Supplementary information for compilation of data), and other seawater constituents that may affect Fe speciation (e.g. $[H^+]$, $[HS^-]$, [DOC]) are also highly variable (and independent of Fe) in hydrothermal environments. Future studies should aim to scrutinise the speciation of Fe in a range of environments, with a key example being the Rainbow site, Mid Atlantic Ridge, where fluid Fe = 24 mM (Douville et al., 2002) (cf. this study Fe = 0.8–1.3 mM).

5. Conclusions

We have shown that two fairly typical hydrothermal plumes contained high concentrations of labile Fe that was bound by ligand phases averaging 30% of the DFe concentration or 7.5% of the total hydrothermal Fe. The two vent sites were not statistically different in terms of K'_{FeL} or the ratio of L:DFe, possibly suggesting that certain features of Fe stabilisation in hydrothermal plumes are universal to typical hydrothermal systems. The complexes (along with observed colloidal phases) are likely to remain dissolved and be available for transport into the deep ocean.

Our results suggest that the Fe binding observed was the result of the flocculation of hydrothermal Fe with ambient dissolved organic matter upon entry into the cold deep ocean. In principle, this process may occur in other systems where Fe rich water meets organic rich seawater (such as rivers). It is possible that the resulting complexes are too weak to be detected by traditional CLE–ACSV methods, and that the complexes are lower in concentration than total DFe, preventing detection by the forward titration technique. Such phases may make up some of the previously observed weak ligands, and would be present in all seawater with riverine or hydrothermal inputs. These processes may therefore have an important global impact on Fe concentrations and biogeochemistry.

The two study sites were relatively similar in a global context, and ideally sites with high/low Fe, sulphide, acidity, temperature and level of sedimentation should be examined under the same experimental conditions to test our hypothesis that $\sim$7.5% of all hydrothermal Fe is stabilised. Given that the concentration of Fe in hydrothermal fluids does not seem to depend solely on geological features (spreading rate, temperature) or chemical features ($[HS^-]$, $[H^+]$), further measurements of Fe speciation in various vent sites in a variety of geographical locations are required before numerical models of hydrothermal Fe contribution to the oceans can be constrained.

Acknowledgements

We thank the master and crew of the *RRS James Cook* and the pilots and technical team of the ROV *Isis*. We thank D.R.H. Green and R.H. James for providing hydrothermal end-member fluid data and Veerle Huvenne for providing bathymetric maps. We also thank three anonymous reviewers for their helpful and thought-provoking reviews. The cruises were part of the ChEsSo program (NERC Grant NE/DO1249X/1) and the work of J. Hawkes was funded by a Natural Environment Research Council (NERC, UK) Ph.D. Studentship (NE/H524922).

Appendix A. Supplementary information

Supplementary data associated with this article can be found in the online version at http://dx.doi.org/10.1016/j.epsl.2013.05.047.

References

Baker, E.T., Massoth, G.J., Walker, S.L., Embley, R.W., 1993. A method for quantitatively estimating diffuse and discrete hydrothermal discharge. Earth Planet. Sci. Lett. 118, 235–249.

Baker, E.T., Embley, R.W., Walker, S.L., Resing, J.A., Lupton, J.E., Nakamura, K.i., de Ronde, C.E.J., Massoth, G.J., 2008. Hydrothermal activity and volcano distribution along the Mariana Arc. J. Geophys. Res.-Solid Earth 113 (B8).

Baker, E.T., Massoth, G.J., 1987. Characteristics of hydrothermal plumes from 2 vent fields on the Juan-de-Fuca ridge, Northeast Pacific Ocean. Earth Planet. Sci. Lett. 85, 59–73.

Bennett, S.A., Achterberg, E.P., Connelly, D.P., Statham, P.J., Fones, G.R., German, C.R., 2008. The distribution and stabilisation of dissolved Fe in deep-sea hydrothermal plumes. Earth Planet. Sci. Lett. 270, 157.

Bennett, S.A., Statham, P.J., Green, D.R.H., Le Bris, N., McDermott, J.M., Prado, F., Rouxel, O.J., Von Damm, K., German, C.R., 2011. Dissolved and particulate organic carbon in hydrothermal plumes from the East Pacific Rise, 9 degrees 50°N. Deep-Sea Res. Part I-Oceanogr. Res. Pap. 58, 922–931.

Bennett, S.A., Coleman, M., Huber, J.A., et al., 2013. Trophic regions of a hydrothermal plume dispersing away from an ultramafic-hosted vent-system: Von Damm vent-site, Mid-Cayman Rise. Geochem. Geophys. Geosyst. 14 (2), 317–327.

Benoit, G., Oktaymarshall, S.D., Cantu, A., Hood, E.M., Coleman, C.H., Corapcioglu, M. O., Santschi, P.H., 1994. Partitioning of Cu, Pb, Ag, Zn, Fe, Al, and Mn between filter-retained particles, colloids, and solution in 6 Texas estuaries. Mar. Chem. 45, 307–336.

Bergquist, B.A., Wu, J., Boyle, E.A., 2007. Variability in oceanic dissolved iron is dominated by the colloidal fraction. Geochim. Cosmochim. Acta 71, 2960–2974.

Boye, M., van den Berg, C.M., de Jong, J., Leach, H., Croot, P., de Baar, H.J., 2001. Organic complexation of iron in the Southern Ocean. Deep Sea Research Part I: Oceanographic Research Papers 48 (6), 1477–1497.

Boye, M., Nishioka, J., Croot, P., Laan, P., Timmermans, K.R., Strass, V.H., Takeda, S., de Baar, H.J.W., 2010. Significant portion of dissolved organic Fe complexes in fact is Fe colloids. Mar. Chem. 122, 20–27.

Boye, M., Nishioka, J., Croot, P.L., Laan, P., Timmermans, K.R., de Baar, H.J.W., 2005. Major deviations of iron complexation during 22 days of a mesoscale iron enrichment in the open southern ocean. Mar. Chem. 96, 257–271.

Boyle, E., Jenkins, W., 2008. Hydrothermal iron in the deep western South Pacific. Geochim. Cosmochim. Acta 72, A107. 8th Annual V M Goldschmidt Conference, Vancouver, Canada, July 2008.

Breier, J.A., Toner, B.M., Fakra, S.C., Marcus, M.A., White, S.N., Thurnherr, A.M., German, C.R., 2012. Sulfur, sulfides, oxides and organic matter aggregated in submarine hydrothermal plumes at 9 degrees 50°N East Pacific Rise. Geochim. Cosmochim. Acta 88, 216–236.

Bruguier, N.J., Livermore, R.A, 2001. Enhanced magma supply at the southern East Scotia Ridge: evidence for mantle flow around the subducting slab? Earth Planet. Sci. Lett. 191, 129–144.

Bruland, K.W., Franks, R.P., Knauer, G.A., Martin, J.H., 1979. Sampling and analytical methods for the determination of copper, cadmium, zinc, and nickel at the nanogram per liter level in seawater. Anal. Chim. Acta 105, 233–245.

Butterfield, D., Massoth, G., 1994. Geochemistry of north cleft segment vent fluids—temporal changes in chlorinity and their possible relation to recent volcanism. J. Geophys. Res.-Solid Earth 99, 4951–4968.

Campbell, A., Bowers, T., Measures, C., Falkner, K., Khadem, M., Edmond, J., 1988. A time-series of vent fluid compositions from 21-degrees-N, East Pacific Rise (1979, 1981, 1985), and the Guaymas Basin, Gulf of California (1982, 1985). J. Geophys. Res.-Solid Earth Planets 93, 4537–4549.

Chen, M., Wang, W.X., 2004. Phase partitioning and solubility of iron in natural seawater controlled by dissolved organic matter. Global Biogeochem. Cycles 18, GB4013.

Coombs, D.S., Landis, C.A., 1966. Pumice from the south sandwich eruption of march 1962 reaches New Zealand. Nature 209, 289–290.

Cowen, J.P., Li, Y.H., 1991. The influence of a changing bacterial community on trace metal scavenging in a deep-sea particle plume. J. Mar. Res. 49, 517–542.

Croot, P.L., Andersson, K., Ozturk, M., Turner, D.R., 2004. The distribution and specification of iron along 6 degrees E in the southern ocean. Deep-Sea Res. Part II-Top. Stud. Oceanogr. 51, 2857–2879.

Croot, P.L., Heller, M.I., 2012. The importance of kinetics and redox in the biogeochemical cycling of iron in the surface ocean. Front. Microbiol. 3.

Croot, P.L., Johansson, M., 2000. Determination of iron speciation by cathodic stripping voltammetry in seawater using the competing ligand 2-(2-thiazolylazo)-p-cresol (TAC). Electroanalysis 12, 565–576.

Cullen, J.T., Bergquist, B.A., Moffett, J.W., 2006. Thermodynamic characterization of the partitioning of iron between soluble and colloidal species in the Atlantic Ocean. Mar. Chem. 98, 295–303.

Davies, S., Morgan, J., 1989. Manganese(II) oxidation kinetics on metal oxide surfaces. J. Colloid Interface Sci. 129, 63–77.

De Angelis, M.A., Lilley, M.D., Olson, E.J., Baross, J.A., 1993. Methane oxidation in deep-sea hydrothermal plumes of the endeavor segment of the Juan-de-Fuca ridge. Deep-Sea Res. Part I-Oceanogr. Res. Pap. 40 (6), 1169–1186.

De Baar, H.J.W., De Jong, J.T.M., 2001. Distributions, sources and sinks of iron in seawater. In: Turner, D.R., Hunter, K.A. (Eds.), The Biogeochemistry of Iron in Seawater. IUPAC Series on Analytical and Physical Chemistry of Environmental Systems. John Wiley & Sons Ltd., Chichester, pp. 123–253.

de Ronde, C., Baker, E., Massoth, G., Lupton, J., Wright, I., Feely, R., Greene, R., 2001. Intra-oceanic subduction-related hydrothermal venting, Kermadec volcanic arc, New Zealand. Earth Planet. Sci. Lett. 193 (3–4), 359–369.

Dick, G.J., Clement, B.G., Webb, S.M., Fodrie, F.J., Bargar, J.R., Tebo, B.M., 2009. Enzymatic microbial Mn(II) oxidation and Mn biooxide production in the Guaymas Basin deep-sea hydrothermal plume. Geochim. Cosmochim. Acta 73, 6517–6530.

Douville, E., Charlou, J.L., Oelkers, E.H., Bienvenu, P., Colon, C.F.J., Donval, J.P., Fouquet, Y., Prieur, D., Appriou, P., 2002. The rainbow vent fluids (36 degrees 14°N, MAR): the influence of ultramafic rocks and phase separation on trace metal content in Mid-Atlantic Ridge hydrothermal fluids. Chem. Geol. 184, 37–48.

Edmonds, H., German, C., 2004. Particle geochemistry in the Rainbow hydrothermal plume, Mid-Atlantic Ridge. Geochim. Cosmochim. Acta 68, 759–772.

Elderfield, H., Schultz, A., 1996. Mid-ocean ridge hydrothermal fluxes and the chemical composition of the ocean. Annu. Rev. Earth Planet. Sci. 24, 191–224.

Farley, K.J., Morel, F.M.M., 1986. Role of coagulation in the kinetics of sedimentation. Environ. Sci. Technol. 20, 187–195.

Feely, R., Lewison, M., Massoth, G., Robertbaldo, G., Lavelle, J., Byrne, R., Vondamm, K., Curl, H., 1987. Composition and dissolution of black smoker particulates from active vents on The Juan-De-Fuca Ridge. J. Geophys. Res.-Solid Earth Planets 92, 11347–11363.

Field, M.P., Sherrell, R.M., 2000. Dissolved and particulate Fe in a hydrothermal plume at 9 degrees 45°N, east pacific rise: slow Fe (II) oxidation kinetics in pacific plumes. Geochim. Cosmochim. Acta 64 (4), 619–628.

Gallant, R.M., Von Damm, K.L., 2006. Geochemical controls on hydrothermal fluids from the Kairei and Edmond vent fields, 23 degrees–25 degrees S, Central Indian Ridge. Geochem. Geophys. Geosyst. 7, 24.

German, C.R., Campbell, A.C., Edmond, J.M., 1991. Hydrothermal scavenging at the Mid-Atlantic Ridge—modification of trace-element dissolved fluxes. Earth Planet. Sci. Lett. 107, 101–114.

German, C.R., Klinkhammer, G.P., Edmond, J.M., Mitra, A., Elderfield, H., 1990. Hydrothermal scavenging of rare-earth elements in the ocean. Nature 345, 516–518.

German, C.R., Thurnherr, A.M., Knoery, J., Charlou, J.L., Jean-Baptiste, P., Edmonds, H.N., 2010. Heat, volume and chemical fluxes from submarine venting: a synthesis of results from the rainbow hydrothermal field, 36°N MAR. Deep–Sea Res. I 57, 518–527.

German, C.R., Von Damm, K.L., 2004. Hydrothermal processes. In: Holland, H., Turekian, K. (Eds.), The Oceans and Marine Geochemistry, vol. 6. Elsevier-Pergamon, Oxford, pp. 181–222.

Gerringa, L.J.A., Rijkenberg, M.J.A., Wolterbeek, H.T., Verburg, T.G., Boye, M., deBaar, H.J.W., 2007. Kinetic study reveals weak Fe-binding ligand, which affects the solubility of Fe in the Scheldt estuary. Mar. Chem. 103, 30–45.

Gledhill, M., van den Berg, C., Nolting, R., Timmermans, K., 1998. Variability in the speciation of iron in the northern North Sea. Mar. Chem. 59, 283–300.

Gledhill, M., van den Berg, C.M.G., 1994. Determination of complexation of iron(III) with natural organic complexing ligands in seawater using cathodic stripping voltammetry. Mar. Chem. 47, 41–54.

Gledhill, M., Buck, K.N., 2012. The organic complexation of iron in the marine environment: a review. Front. Microbiol. 3, 69.

Hassler, C.S., Legiret, F., Butler, E.C.V., 2013. Measurement of iron chemical speciation in seawater at 4 °C: the use of competitive ligand exchange–adsorptive cathodic stripping voltammetry. Mar. Chem. 149, 63–73.

Hawkes, J.A., Gledhill, M., Connelly, D.P., Achterberg, E.P., 2013. Characterisation of iron binding ligands in seawater by reverse titration. Anal. Chim. Acta 766, 53–60.

Hiemstra, T., van Riemsdijk, W.H., 2006. Biogeochemical speciation of Fe in ocean water. Mar. Chem. 102, 181–197.

Honeyman, B.D., Santschi, P.H., 1989. A brownian-pumping model for oceanic trace metal scavenging—evidence from Th-isotopes. J. Mar. Res. 47, 951–992.

Honeyman, B.D., Santschi, P.H., 1991. Coupling adsorption and particle aggregation—laboratory studies of colloidal pumping using Fe-59 labeled hematite. Environ. Sci. Technol. 25, 1739–1747.

Hunter, K.A., Boyd, P.W., 2007. Iron-binding ligands and their role in the ocean biogeochemistry of iron. Environ. Chem. 4, 221–232.

Hunter, K.A., Liss, P.S., 1982. Organic matter and the surface charge of suspended particles in estuarine waters. Limnol. Oceanogr. 27, 322–335.

James, R.H., Green, D.R. H., Stock, M.J., Connelly, D.P., Alker, B.J., Banerjee, N., Cole, C., German, C.R., Huvenne, V.A.I. Powell, A., Geochemistry of hydrothermal fluids and associated mineralisation on the East Scotia Ridge, (in prep.).

Karl, D.M, 1995. The Microbiology of Deep-Sea Hydrothermal Vents. Extreme and Unusual Environments. CRC Press Inc., Roca Raton, FL.

Klevenz, V., Bach, W., Schmidt, K., Hentscher, M., Koschinsky, A., Petersen, S., 2011. Geochemistry of vent fluid particles formed during initial hydrothermal fluid–seawater mixing along the Mid-Atlantic Ridge. Geochem. Geophys. Geosyst. 12 (10).

Klinkhammer, G., Elderfield, H., Greaves, M., Rona, P., Nelsen, T., 1986. Manganese geochemistry near high-temperature vents in the Mid-Atlantic Ridge rift-valley. Earth Planet. Sci. Lett. 80, 230–240.

Klunder, M.B., Laan, P., Middag, R., De Baar, H.J.W., van Ooijen, J.C., 2011. Dissolved iron in the Southern Ocean (Atlantic sector). Deep-Sea Res. Part I-Oceanogr. Res. Pap. 58, 2678–2694.

Kondo, Y., Takeda, S., Furuya, K., 2012. Distinct trends in dissolved Fe speciation between shallow and deep waters in the Pacific Ocean. Mar. Chem. 134–135, 18–28.

Laglera, L.M., van den Berg, C.M.G., 2009. Evidence for geochemical control of iron by humic substances in seawater. Limnol. Oceanogr. 54, 610–619.

Lang, S.Q., Butterfield, D.A., Lilley, M.D., 2006. Dissolved organic carbon in ridge-axis and ridge-flank hydrothermal systems. Geochim. Cosmochim. Acta 70, 3830.

Lewis, E., Wallace, D.W.R., 1998. Program Developed for CO_2 System Calculations. Carbon Dioxide Information Analysis Center, Oak Ridge National Laboratory, U. S. Department of Energy, Oak Ridge, TN, USA.

Liu, X., Millero, F.J., 2002. The solubility of iron in seawater. Mar. Chem. 77, 43.
Loscher, B.M., DeBaar, H.J.W., DeJong, J.T.M., Veth, C., Dehairs, F., 1997. The distribution of Fe in the Antarctic Circumpolar Current. Deep–Sea Res. Part II: Top. Stud. Oceanogr. 44, 143–187.
Lupton, J., Delaney, J., Johnson, H., Tivey, M., 1985. Entrainment and vertical transport of deep-ocean water by buoyant hydrothermal plumes. Nature 316, 621–623.
Luther, G., Rickard, D., 2005. Metal sulfide cluster complexes and their biogeochemical importance in the environment. J. Nanoparticle Res. 7, 389–407.
Luther, G.W., Ferdelman, T.G., 1993. Voltammetric characterization of iron(II) sulfide complexes in laboratory solutions and in marine waters and porewaters. Environ. Sci. Technol. 27, 1154–1163.
Luther, G.W., Rickard, D.T., Theberge, S., Olroyd, A., 1996. Determination of metal (bi)sulfide stability constants of Mn^{2+}, Fe^{2+}, Co^{2+}, Ni^{2+}, Cu^{2+} and Zn^{2+} by voltammetric methods. Environ. Sci. Technol. 30, 671–679.
Mackey, D., Zirino, A., 1994. Comments on trace-metal speciation in seawater or do onions grow in the sea. Anal. Chim. Acta 284, 635–647.
Marshall, J., Speer, K., 2012. Closure of the meridional overturning circulation through Southern Ocean upwelling. Nat. Geosci. 5, 171–180.
Martin, J.H., Fitzwater, S.E., 1988. Iron-deficiency limits phytoplankton growth in the northeast Pacific subarctic. Nature 331, 341–343.
Millero, F.J., Woosley, R., Ditrolio, B., Waters, J., 2009. Effect of ocean acidification on the speciation of metals in seawater. Oceanography 22, 72–85.
Moore, J.K., Braucher, O., 2008. Sedimentary and mineral dust sources of dissolved iron to the world ocean. Biogeosciences 5, 631–656.
Mosley, L.M., Hunter, K.A., Ducker, W.A., 2003. Forces between colloid particles in natural waters. Environ. Sci. Technol. 37, 3303–3308.
Mottl, M.J., McConachy, T.F., 1990. Chemical processes in buoyant hydrothermal plumes on the east pacific rise near 21-degrees-n. Geochim. Cosmochim. Acta 54, 1911–1927.
Naveira-Garabato, A., Heywood, K., Stevens, D., 2002. Modification and pathways of Southern Ocean Deep Waters in the Scotia Sea. Deep-Sea Res. Part I-Oceanogr. Res. Pap. 49, 681–705.
Nishioka, J., Takeda, S., de Baar, H.J.W., Croot, P.L., Boye, M., Laan, P., Timmermans, K. R., 2005. Changes in the concentration of iron in different size fractions during an iron enrichment experiment in the open southern ocean. Mar. Chem. 95, 51–63.
Nishioka, J., Obata, H., Tsumune, D., 2013. Evidence of an extensive spread of hydrothermal dissolved iron in the Indian Ocean. Earth Planet. Sci. Lett. 361, 26–33.
Nolting, R.F., De Baar, H.J.W., Van Bennekom, A.J., Masson, A., 1991. Cadmium, copper and iron in the Scotia sea, Weddell Sea and Weddell/Scotia confluence (Antarctica). Mar. Chem. 35, 219–243.
Nuester, J., van den Berg, C.M.G., 2005. Determination of metal speciation by reverse titrations. Anal. Chem. 77, 11–19.
Risso, C., Scasso, R.A., Aparicio, A., 2002. Presence of large pumice blocks on Tierra del Fuego and South Shetland Islands shorelines, from 1962 South Sandwich Islands eruption. Mar. Geol. 186, 413.
Rogers, A.D., Tyler, P.A., Connelly, D.P., Copley, J.T., James, R., Larter, R.D., Linse, K., Mills, R.A., Garabato, A.N., Pancost, R.D., Pearce, D.A., Polunin, N.V.C., German, C. R., Shank, T., Boersch-Supan, P.H., Alker, B.J., Aquilina, A., Bennett, S.A., Clarke, A., Dinley, R.J.J., Graham, A.G.C., Green, D.R.H., Hawkes, J.A., Hepburn, L., Hilario, A., Huvenne, V.A.I., Marsh, L., Ramirez-Llodra, E., Reid, W.D.K., Roterman, C.N., Sweeting, C.J., Thatje, S., Zwirglmaier, K., 2012. The discovery of new deep-sea hydrothermal vent communities in the southern ocean and implications for biogeography. PLoS Biol. 10, e1001234.
Rue, E.L., Bruland, K.W., 1995. Complexation of Fe(III) by natural organic ligands in the central north pacific as determined by a new competitive ligand equilibration adsorptive cathodic stripping voltammetric method. Mar. Chem. 50, 117–138.
Sander, S.G., Koschinsky, A., 2011. Metal flux from hydrothermal vents increased by organic complexation. Nat. Geosci. 4, 145–150.
Sands, C.M., Connelly, D.P., Statham, P.J., German, C.R., 2012. Size fractionation of trace metals in the Edmond hydrothermal plume, Central Indian Ocean. Earth Planet. Sci. Lett. 319, 15–22.
Sañudo-Wilhelmy, S.A., Rivera-Duarte, I., Flegal, A.R., 1996. Distribution of colloidal trace metals in the San Francisco Bay estuary. Geochim. Cosmochim. Acta 60, 4933–4944.
Schlosser, C., De La Rocha, C.L., Croot, P.L., 2011. Effects of iron surface adsorption and sample handling on iron solubility measurements. Mar. Chem. 127 (1–4), 48–55.
Schlosser, C., De La Rocha, C.L., Streu, P., Croot, P.L., 2012. Solubility of iron in the Southern Ocean. Limnol. Oceanogr. 57 (3), 684–697.
Shi, D., Xu, Y., Hopkinson, B.M., Morel, F.M.M., 2010. Effect of ocean acidification on iron availability to marine phytoplankton. Science 327, 676–679.
Statham, P.J., German, C.R., Connelly, D.P., 2005. Iron (II) distribution and oxidation kinetics in hydrothermal plumes at the Kairei and Edmond vent sites, Indian Ocean. Earth Planet. Sci. Lett. 236, 588.
Statham, P.J., Jacobson, Y., van den Berg, C.M.G., 2012. The measurement of organically complexed Fe-II in natural waters using competitive ligand reverse titration. Anal. Chim. Acta 743, 111–116.
Stockdale, A., Tipping, E., Hamilton-Taylor, J., Lofts, S., 2011. Trace metals in the open oceans: speciation modelling based on humic-type ligands. Environ. Chem. 8, 304–319.
Sutherland, F.L., 1965. Dispersal of pumice, supposedly from the 1962 South Sandwich Islands eruption, on Southern Australian shores. Nature 207, 1332–1335.
Tagliabue, A., Bopp, L., Dutay, J.C., Bowie, A.R., Chever, F., Jean-Baptiste, P., Bucciarelli, E., Lannuzel, D., Remenyi, T., Sarthou, G., Aumont, O., Gehlen, M., Jeandel, C., 2010. Hydrothermal contribution to the oceanic dissolved iron inventory. Nat. Geosci. 3, 252–256.
Toner, B.M., Kafra, S.C., Manganini, S.J., 2009. Preservation of iron(II) by carbon-rich matrices in a hydrothermal plume. Nat. Geosci. 2, 197.
Turner, J., 1973. Buoyancy Effects in Fluids. Cambridge University Press.
Ussher, S.J., Achterberg, E.P., Sarthou, G.R., Laan, P., de Baar, H.J.W., Worsfold, P.J., 2010. Distribution of size fractionated dissolved iron in the canary basin. Mar. Environ. Res. 70, 46–55.
Wang, H., Yang, Q., Ji, F., Lilley, M.D., Zhou, H., 2012. The geochemical characteristics and Fe(II) oxidation kinetics of hydrothermal plumes at the Southwest Indian Ridge. Mar. Chem. 134, 29–35.
Witter, A.E., Hutchins, D.A., Butler, A., Luther, G.W., 2000. Determination of conditional stability constants and kinetic constants for strong model Fe-binding ligands in seawater. Mar. Chem. 69, 1–17.
Wu, J., Boyle, E., Sunda, W., Wen, L.S., 2001. Soluble and colloidal iron in the oligotrophic North Atlantic and North Pacific. Science 293, 847–849.
Wu, J., Luther, G.W., 1995. Complexation of Fe(III) by natural organic ligands in the north-west Atlantic Ocean by a competitive ligand equilibration method and a kinetic approach. Mar. Chem. 50, 159–177.
Wu, J., Wells, M.L., Rember, R., 2011. Dissolved iron anomaly in the deep tropical–subtropical Pacific: evidence for long-range transport of hydrothermal iron. Geochim. Cosmochim. Acta 75, 460–468.
Yucel, M., Gartman, A., Chan, C.S., Luther, G., 2011. Hydrothermal vents as a kinetically stable source of iron-sulphide-bearing nanoparticles to the ocean. Nat. Geosci. 4, 367–371.